Journal of the European Ceramic Society 15 (1995) 689–695

0955-2219(95)00026-7
0955-2219/95/$9.50

Study on the Solid Solubility of Al in the Melilite Systems $R_2Si_{3-x}Al_xO_{3+x}N_{4-x}$ with R = Nd, Sm, Gd, Dy and Y

P. L. Wang,[a] H. Y. Tu,[a] W. Y. Sun,[a] D. S. Yan,[a] M. Nygren[b] & T. Ekström[b]

[a]The State Key Lab. on High Performance Ceramics and Superfine Microstructure, Shanghai Institute of Ceramics, Chinese Academy of Sciences, Shanghai 200050, P. R. China
[b]Dept. of Inorg. Chemistry, University of Stockholm, S-106 91 Stockholm, Sweden

(Received 28 September 1994; revised version received 12 January 1995; accepted 31 January 1995)

Abstract

The solubility of aluminium in the nitrogen-containing melilite structure has been studied by preparation of specimens of the general formula $R_2Si_{3-x}Al_xO_{3+x}N_{4-x}$ with R = Nd, Sm, Gd, Dy and Y by hot pressing and pressureless sintering techniques in the temperature interval 1600–1750°C. For elements with large ionic radii, i.e. R = Nd and Sm, up to one Si can be replaced by Al, but the solubility limits in melilite solid solutions decrease with decreasing the ionic radii. Consequently, yttrium–melilite had the lowest observed aluminium solubility ($x \approx 0{\cdot}6$) in rare earth elements–melilite solid solutions.

1 Introduction

Nitrogen-containing melilite phases comprise compounds based on the general melilite composition $Si_3N_4{\cdot}R_2O_3$ with R = Y, and rare earth elements such as Nd, Sm, Gd and Dy, and these compounds have been shown to be refractory and stable ceramics in non-oxidising environments. Yttria and rare earth oxides are frequently used as a sintering aid in the preparation of Sialon ceramics. Consequently nitrogen-containing melilite phases are frequently occurring as a grain boundary phase in α-Sialon and mixed α–β-Sialon ceramics.[1,2] This is expected from phase relationships of the R–Si–Al–O–N systems[3,4] and, apart from the α-Sialon phase, these phases contain more nitrogen than any other phase in these quinary systems. By the formation of crystalline nitrogen-containing rare earth element–melilite (abbreviated R–M below) and/or aluminium and nitrogen-containing rare earth element–melilite solid solution (abbreviated R–M' below) phases, the amount of glassy phase at the grain boundary is reduced and eventually totally eliminated. The ability of the various R–M' phases to act as 'element sink phases' will be discussed below.

The properties of Sialon ceramics at high temperatures are mainly determined by the deterioration of the grain boundary phase. The presence of Y–M in silicon nitride based ceramics has been avoided. Y–M is known to oxidise rapidly at low temperatures (around 1000°C) whereby cristobalite and yttrium disilicate is formed and this process is accompanied with a drastic increase in the specific volume. The specific volume of the latter phases is thus approximately 30% larger than that of Y–M resulting in cracking of the specimen and spalling of the protective oxide layer formed upon oxidation.[5] Thus, although the melting point of Y–M itself is very high (>1850°C) these materials have failed in high-temperature application due to their poor oxidation resistance.[6] Aluminium melilite solid solutions $R_2Si_{3-x}Al_xO_{3+x}N_{4-x}$(R–M') are expected to have an improved stability against oxidation because when Si–N is replaced by Al–O a much smaller relative increase in specific volume of the formed oxidation products is expected and can be used as the best high temperature grain boundary phases for mixed α–β-Sialon ceramics because of their high melting points. Sialon ceramics containing crystalline R–M' phases at the grain boundaries are thus expected to exhibit better oxidation properties than the corresponding materials containing crystalline R–M phases.

The aluminium solid solution range in the Nd–M' system is reported to extend from $Nd_2Si_3O_3N_4$ to around $Nd_2Si_2AlO_4N_3$.[6,7] This range is very similar to the one reported for the Sm–M' system where, also, up to one Si can be replaced by one Al.[8] In order to understand the characteristics of the oxidation behaviour of various R–M' phases, it is necessary, at the first stage, to study

the extension of solubility range of the R–M' phases and the microstructure of the formed compacts and this is reported below.

2 Experimental

The starting powders used were silicon nitride (LC12, H. C. Starck, Berlin) and aluminium nitride (prepared at Shanghai Institute of Ceramics) while R_2O_3 with R = Nd, Sm, Gd, Dy and Y (99·9% pure) were all the products of Yaolung Chemical Works, China. Powder mixtures with the overall nominal composition $R_2Si_{3-x}Al_xO_{3+x}N_{4-x}$ with R = Nd, Sm, Gd, Dy and Y and $0 \leq x \leq 1{\cdot}5$, taking into account surface oxygen of the particles of both Si_3N_4 (1·8 wt%) and AlN (2·0 wt%), were prepared. The powders were mixed in absolute alcohol and milled in an agate mortar for 1·5 h. The compacted samples were fired at the different temperatures in the interval 1600–1750°C for 1 h or 2 h depending on the nominal composition of R–M' to have the samples synthesized, applying both hot-pressing or pressureless sintering techniques in a graphite-resistance furnace in a flowing nitrogen atmosphere.

The phase analysis of the prepared samples was based on X-ray diffraction data obtained in a Guinier–Hägg camera with use of Cu $K\alpha_1$ radiation and Si as the internal standard. The obtained photographs were evaluated with a computerised scanner system and the cell parameters were refined with use of the program PIRUM.[9] The Al content of the prepared R–M' phases were determined from element analysis using either an SEM (Jeol JSM 820) and a TEM (JEM 200CX), both equipped with energy dispersive spectrometers, or an electron probe instrument (8705 QH2). The Si and Al content given below is an average of several (10 or more) spot analysis determinations. The micrographs were obtained in an SEM (Jeol JSM 820) operating in the back scattering mode. The detailed microstructural studies of Sm–, Gd– and DY–M' samples were made in a TEM (JEM 200CX).

3 Results and Discussion

3.1 Phase analysis

The observed crystalline phases in the prepared samples are given in Table 1. The results are given

Table 1. A summary of the phases present in $R_2Si_{3-x}Al_xO_{3+x}N_{4-x}$ compacts according to the X-ray analysis

Sample	*Nominal x value*	*Firing condition (°C/h)*	*Phases present*						
			M	*M'*	*J*	*K*	*H(S)*	*I(Y)*	*A*
	0	1700/1 HP	vs			vw			
	0·5	1700/2 PLS		vs	tr				
Nd–M'	0·75	1700/2 PLS		vs	tr		tr		
	1·0	1700/1 HP		vs	tr		tr		
	1·25	1675/1 HP		vs	vw			w	
	0	1750/1 HP	vs				(vw)		
	0·3	1750/1 HP		vs	tr				
	0·5	1700/2 PLS		vs	tr				
Sm–M'	0·75	1700/2 PLS		vs	vw				
	1·0	1700/1 HP		vs	vw				
	1·5	1600/1 HP		vs	vw			m	
	0	1700/1 HP	vs		vw				
	0·3	1700/1 HP		vs	vw				
Gd–M'	0·5	1750/2 PLS		vs	vw				
	0·75	1700/1 HP		vs	vw				
	1·0	1700/2 PLS		vs	w				
	1·5	1600/1 PLS		vs	vw			ms	
	0	1700/1 HP	vs		vw				
	0·4	1700/1 HP		vs	w				
Dy–M'	0·6	1750/2 PLS		vs	w				
	0·75	1700/1 HP		vs	w				
	1·0	1700/2 PLS		vs	w				
	1·5	1600/1 PLS		vs	w			(ms)	
	0	1750/1 HP	vs		w				
	0·375	1700/1 HP		vs	w				
Y–M'	0·6	1700/1 HP		vs	w				
	1·0	1700/1 HP		vs	mw				tr
	1·25	1700/1 HP		vs	m				w

HP = hot pressing; PLS = pressureless sintering; J = $R_4Si_2O_7N_2$; K = $R_3Si_3O_6N_3$; H = $R_{10}(SiO_4)_6N_2$; S = $R_2Si_2O_7$; I = $RAlO_3$; Y = $Al_5Dy_3O_{12}$; A = AlN-polytypoid.

as a function of the x value of the overall compositions $R_2Si_{3-x}Al_xO_{3+x}N_{4-x}$ with R = Nd, Sm, Gd, Dy and Y and $x \leq 1{\cdot}5$ and as expected the R–M phase or the R–M' phase was found to be the main phase in all samples, but the formed samples contained other phases as well. Thus minor amounts of $Nd_3Si_3O_6N_3$ (Nd–K phase) and $Sm_2Si_2O_7$ was found for $x = 0$ in these systems and trace amounts of $Nd_{10}(SiO_4)_6N_2$ appeared in the Nd–M' system. The J phase, $R_4Si_2O_7N_2$ (or corresponding J'-phase), was found in most other samples. For a given nominal composition, the amount of J phase increased with decreasing the ionic radii of the rare earth element. Finally, the synthesis of Yb–M with the composition $Yb_2O_3{\cdot}Si_3N_4$ was tried by hot-pressing at 1700°C for 1 h and the sample contained the Yb–J phase, $Yb_4Si_2O_7N_2$, as a major component and only minor amounts of Yb–M, which in turn suggests that the R–M' phase is more easily formed for the high ionic radii (low Z) rare earth elements.

In addition, $RAlO_3$ was observed in samples of Nd–M', Sm–M' and Gd–M' with $x > 1{\cdot}0$ while $Al_5Dy_3O_{12}$ was found in samples of Dy–M'. Small amounts of AlN-polytypoid (27R or 2H[6]) appeared in the Y–M' material for $x \geq 1$, which was also confirmed by the SEM/EDS studies (see below).

The occurrence of small amounts of additional phases in samples with $x = 0$ might be attributed to the presence of surface oxide on the silicon nitride powder, which cannot be compensated for at this specific composition. However, we have not been able to prepare monophasic R-M' phases, although these compositions have been compensated for surface oxides on the nitride particles. This can be understood for two reasons. Firstly, the densification process of melilite phase would be the same as Si_3N_4-based ceramics because its composition consists of Si_3N_4 and R_2O_3, i.e. the formation of an oxynitride liquid due to the reaction of rare earth oxides with the silica present on the starting nitrogen-containing powder is an important feature of the densification process, which results in the occurrence of amorphous or crystalline intergranular phases after sintering in R–M/R–M' samples. Secondly, the overall compositions might still be in an oxygen-rich multiphase region, especially for the compositions with high x values. According to the phases analysis, the nominal R–M' compositions with $x > 1{\cdot}0$ and with R = Nd, Sm and Gd might be located in the phase compatible region R–M' – R–J – $RAlO_3$ and for R = Dy in the region R–M' – R–J – $Al_5Dy_3O_{12}$. It is known that in the pseudo-binary systems R_2O_3 – Al_2O_3 (R = rare earth elements), the aluminate phase $RAlO_3$ is formed for low and middle Z rare earth elements, whereas the phase $Al_5R_3O_{12}$ is formed only for Dy and higher Z rare earth elements.[10,11] This is in analogy to the phases found in the present R–M' samples with $x > 1{\cdot}0$. It can also be noted that in spite of the fact that the ionic radii of Y^{3+} is similar to that of Dy^{3+}, $Al_5Y_3O_{12}$ is not formed but AlN-polytypoids are.

3.2 Solid solubility range of R–M' phases

The variations of the a- and c-axis parameters of the tetragonal unit cell of the formed R–M' phases are given as function of the x values of the $R_2Si_{3-x}Al_xO_{3+x}N_{4-x}$ samples in Table 2. The lattice dimensions increase with increasing x-values up to a certain x-value for respective R–M' phases. However, these x-values do not necessarily represent true solubility limits as all samples contained additional phases some of which are rare earth rich. It can, however, be noted that the c/a ratios are almost constant with increasing x-value for each R–M' phase which indicates that the structural changes introduced when Si–N pairs are replaced by Al–O ones are isotropic in all R–M'-phases studied.

SEM-EDS studies have been used to estimate the solubility limits of Al in the various R–M' phases. The findings are compiled in Table 2 and Fig. 1. The maximum Al-content in the various R–M' phases were x = 0·98, 0·90, 0·78, 0·71 and 0·57 for R = Nd-, Sm-, Gd-, Dy- and Y, respectively. Thus, in Nd–M' and Sm–M' systems we find that one Si–N pair per formula unit can be replaced by one Al–O pair in accordance with previous findings[6–8] while the true solubility limits in the Gd–M' and Dy–M' systems seem to be somewhat less (0·75) and even the smaller in the Y–M' system (0·60). The maximum Al-content in the R–M'-phases clearly decreases with the ionic radii[12] of the R-element (see Fig. 2).

The substitution of Si–N by Al–O in the R–M structure produced a lattice expansion. The maximum value of latice expansion is found in the Nd–M' system (1·66%) and the minimum one in the Y–M' system (0·70%) which in turn is due to the fact that these systems exhibit different solid solubility ranges. The slopes of the curves of cell parameters versus the x-value are slightly different for different dopings as shown for Y– and Sm–M' in Fig. 1.

Although the small number of additional phases occurs in the formed samples as mentioned above, the measurements of cell parameters and SEM-EDS studies can be done without difficulty because R–M/R–M' phases were found to be the main phases in all samples and the additional phases can be easily separated from the melilite phase in the back scattering mode of SEM.

In order to understand why the solid solubility decreases with decreasing ionic radii of the R

Table 2. Unit cell dimensions and EDS results for samples of the composition $R_2Si_{3-x}Al_xO_{3+x}N_{4-x}$

Sample	*Nominal x value*	*Cell dimensions (Å)*			*x-value based on EDS measurements*
		a	*c*	*c/a*	
	0	7·7229	5·0327	0·652	0
	0·5	7·7471	5·0401	0·651	–
Nd–M'	0·75	7·7569	5·0439	0·650	–
	1·0	7·7667	5·0520	0·651	0·98
	1·25	7·7685	5·0558	0·651	0·94
	0	7·6830	4·9888	0·649	0
	0·3	7·7026	4·9942	0·648	0·25
	0·5	7·7104	4·9985	0·648	0·41
Sm–M'	0·75	7·7156	5·0056	0·649	0·63
	1·0	7·7174	5·0090	0·649	0·80
	1·5	7·7234	5·0080	0·648	0·90
	0	7·6512	4·9605	0·648	0
	0·3	7·6770	4·9670	0·648	–
Gd–M'	0·5	7·6779	4·9744	0·648	0·41
	0·75	7·6816	4·9797	0·648	–
	1·0	7·6870	4·9816	0·648	0·78
	1·5	7·6870	4·9780	0·648	–
	0	7·6180	4·9221	0·646	0
	0·4	7·6326	4·9307	0·646	–
Dy–M'	0·6	7·6371	4·9422	0·647	–
	0·75	7·6412	4·9448	0·647	0·71
	1·0	7·6430	4·9450	0·647	0·64
	1·5	7·6470	4·9410	0·646	–
	0	7·6137	4·9147	0·646	0
	0·375	7·6184	4·9218	0·646	0·32
Y–M'	0·6	7·6204	4·9255	0·646	0·38
	1·0	7·6262	4·9327	0·647	0·57
	1·25	7·6261	4·9315	0·646	0·54

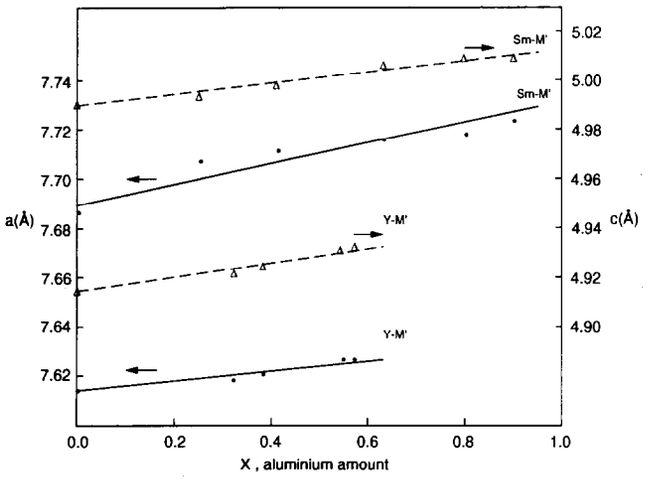

Fig. 1. Variation of the unit cell dimensions plotted vs the actual (SEM-EDS determined) x-values in $R_2Si_{3-x}Al_xO_{3+x}N_{4-x}$ with R = Sm and Y.

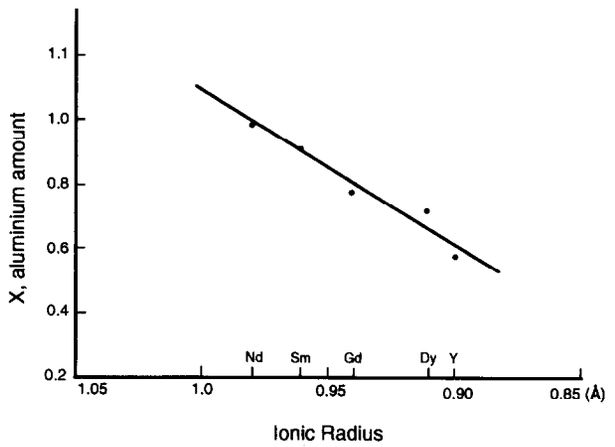

Fig. 2. Maximum solubility of Al in $R_2Si_{3-x}Al_xO_{3+x}N_{4-x}$ plotted vs the ionic radii of the used R element.

element one needs more detailed structural information concerning the metal – non-metal distances of the various R–M' phases. It can, however, be noted that when Si–N is replaced by Al–O the unit cell volume is increased implying that the voids, which accommodate the R element, become larger and eventually they are or will become too large to accommodate the used R element.

3.3 Microstructural studies of compacts containing R–M' phases

The microstructures of R–M' samples containing different amount of Al were studied in an SEM operated in back scattering mode. The micrographs clearly show the multiphase nature of the prepared samples (see in Figs 3 and 4). It is thus clearly seen that large crystals with sharp edges are formed and these crystals are surrounded by a significant

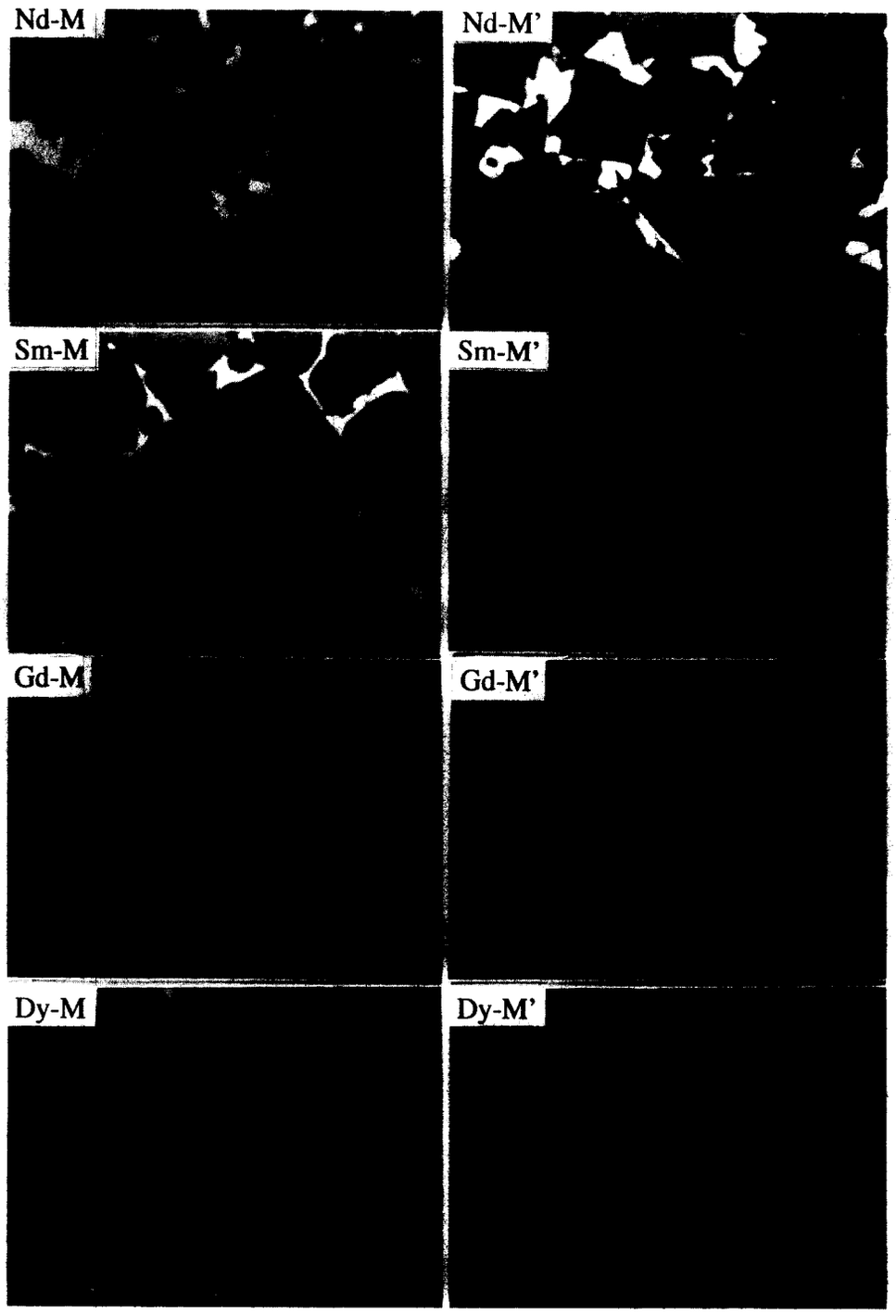

Fig. 3. SEM micrographs of $R_2Si_{3-x}Al_xO_{3+x}N_{4-x}$ with R = Nd, Sm, Gd and Dy and with (a) $x = 0$ and (b) $x = 0{\cdot}5$. The dark grey area represents the R–M' phase and the light grey one the J phase.

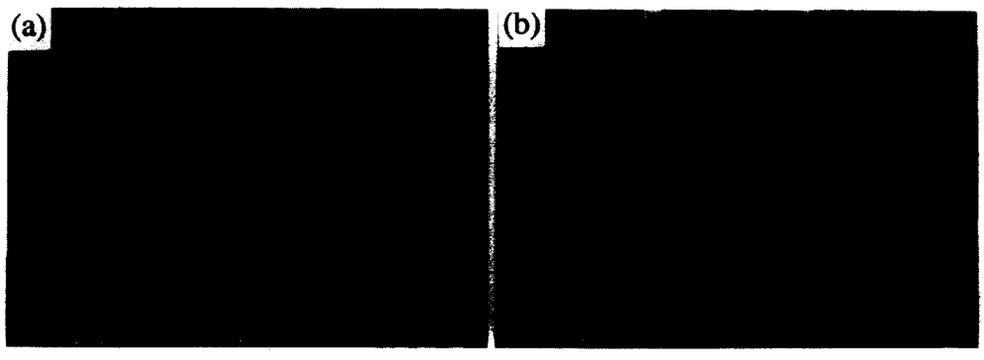

Fig. 4. SEM micrographs of $R_2Si_{3-x}Al_xO_{3+x}N_{4-x}$ with R = Y and with (a) $x = 1{\cdot}0$ and (b) $x = 1{\cdot}25$. The dark grey contrast represents the melilite phase and the light grey one the J phase. The flake and needle-like crystals with black contrast are AlN-polytypoids containing no yttrium.

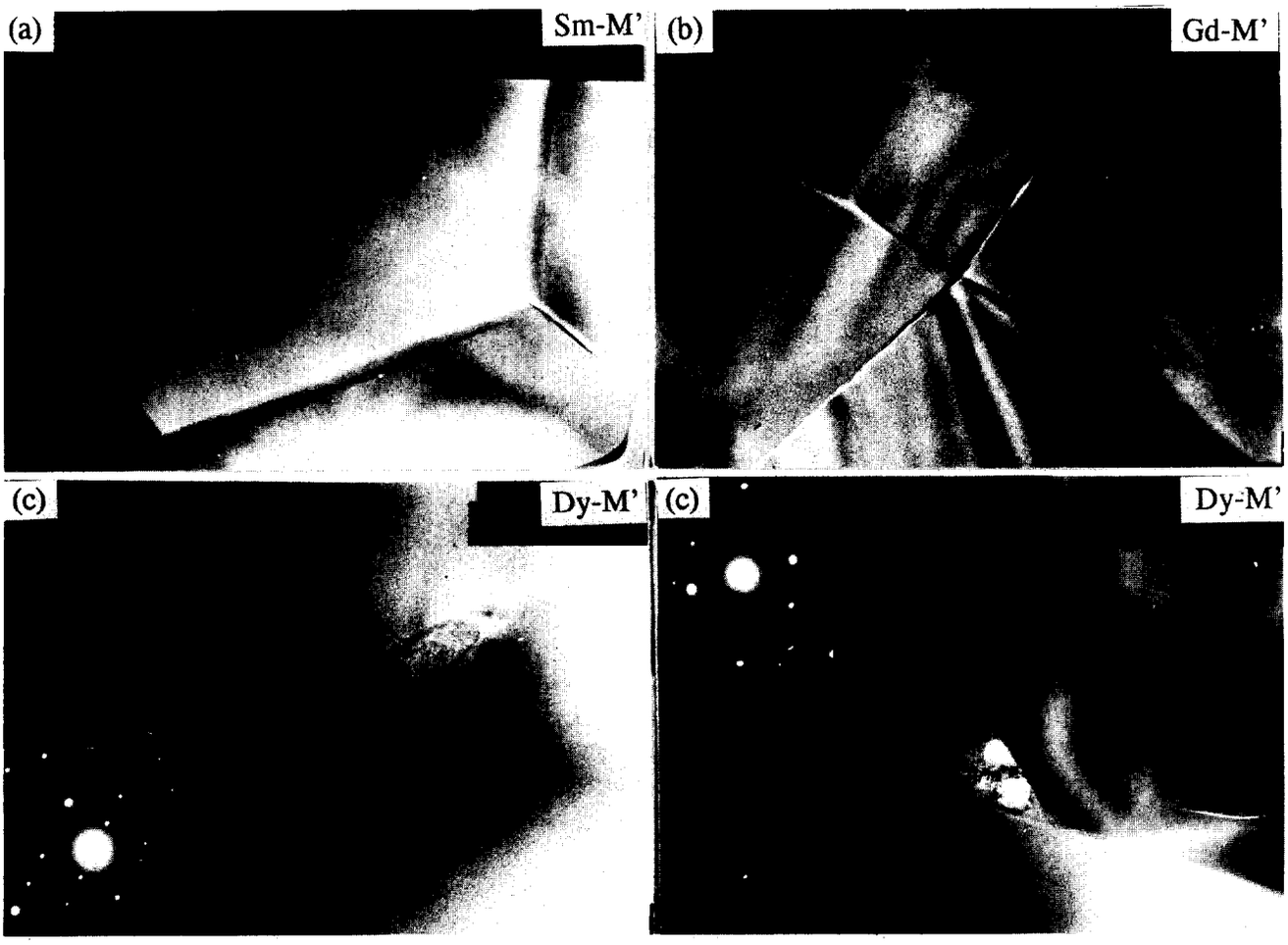

Fig. 5. TEM micrographs of $R_2Si_{3-x}Al_xO_{3+x}N_{4-x}$ samples with (a) R = Sm and x = 0·75, (b) R = Gd and x = 0·5 and (c) R = Dy and x = 0·4.

amount of a rare earth rich grain boundary phase and that the crystallographic morphology of the melilite phase is developed when Si–N are replaced by Al–O in the R–M' samples. This can be understood in terms of the added Al_2O_3 reacting with the silicon oxide on the surface of the nitride particles and with increasing x-value, an increasing amount of liquid phase is formed which in turn promotes the grain growth of the melilite phase.

The SEM micrographs in Fig. 4 show the morphologies of Y–M' phase (dark grey) and J phase (with light grey contrast) in the samples of Y–M' (x = 1·0 and 1·25). The flake and needle-like dark crystals are different AlN-polytypoids containing no yttrium, probably the $2H^{\delta}$ and the 27R modifications respectively. The micrographs also show that the amounts of the J-phase and AlN-polytypoid phases are larger in the sample with x = 1·25 than that of x = 1·0, which agrees with the results of the XRD analysis. The SEM micrographs have revealed that a rare earth element rich grain boundary phase is present in all samples, but more so in the Al containing materials. The XRD analysis has shown that most of it comprises crystalline phases, but the presence of a glassy phase can not be excluded.

TEM studies of triple-grain boundaries in the Sm–M'–(x = 0·75), Gd–M'–(x = 0·5) and Dy–M'–(x = 0·4) samples showed that:

(i) materials prepared with the largest ionic radii element, Sm, exhibited many triple-grain boundaries almost free of any additional phase. Typical triple-grain boundary junctions in this sample are shown in Fig. 5(a);
(ii) in the Gd–M' sample the number of glassy phases in the triple-grain boundaries was increasing but occasionally some multi-grain junctions were observed with no intergranular of glassy phase at all, as shown in Fig. 5(b);
(iii) a mixture of crystalline and glassy phases was always found in the triple-grain boundaries of the Dy–M' material illustrated in the micrographs and electron diffraction patterns given in Fig. 5(c).

These observations are in agreement with the SEM and XRD studies which showed that the homogeneity range of the R–M' phases is largest for the R elements with the largest ionic radii, i.e. these R–M' phases exhibit the best possibility to act as an 'element sink-phase' whereby the amount of glassy phase at the junctions is reduced.

4 Conclusions

The solubility of Al in nitrogen-containing melilite solid solutions according to the formula $R_2Si_{3-x}Al_xO_{3+x}N_{4-x}$ with R = Nd, Sm, Gd, Dy and Y has been studied. The SEM and XRD studies showed that the extension of solid solubility range of the various R–M' phases was largest for the R element with largest ionic radii (Nd and Sm). The TEM studies revealed that the R–M' phase with R = Sm acted as a better 'element sink phase' than R–M' phases containing R elements with smaller ionic radii.

Acknowledgements

The skilful technical assistance of Mrs Y. X. Jia and J. X. Chen is gratefully acknowledged. The State Kay Lab on High Performance Ceramics and Superfine Microstructure, Chinese Academy of Sciences and the Swedish Research Council for Engineering Science are thanked for financial support.

References

1. Wang, P. L., Sun, W. Y. & Yen, T. S., Formation and densification of R-α'-Sialon (R = Nd, Sm, Gd, Dy, Er and Yb). *Mater. Res. Soc. Symp. Proc.*, **287** (1992) 387–92.
2. Persson, J., Ekström, T., Käll, P. O. & Nygren, M., Oxidation behaviour and mechanical properties of β- and mixed α–β Sialons sintered with additions of Y_2O_3 and Nd_2O_3. *J. Eur. Ceram. Soc.*, **11** (1993) 363–73.
3. Huang, Z. K., Tien, T. Y. & Yen, T. S., Subsolidus phase relationships in the Si_3N_4–AlN–rare earth oxide systems. *J. Am. Ceram. Soc.*, **69** (1986) C-241.
4. Sun, W. Y., Tien, T. Y. & Yen, T. S., Subsolidus phase relationships in the part of the system Si, Al, Y/N, O: the system Si_3N_4–AlN–YN–Al_2O_3–Y_2O_3. *J. Am. Ceram. Soc.*, **74** (1991) 2753–8.
5. Patel, J. K. & Thompson, D. P., The low-temperature oxidation problem in yttria-densified silicon nitride ceramics. *Br. Ceram. Trans.*, **87** (1988) 70–3.
6. Slasor, S., Liddel, K. & Thompson, D. P., The role of Nd_2O_3 as an additive in the formation of α' and β' Sialons. *Br. Ceram. Proc.*, **37** (1986) 51–64.
7. Käll, P. -O. & Ekström, T, Sialon ceramics made with mixtures of Y_2O_3–Nd_2O_3 as sintering aids. *J. Eur. Ceram. Soc.*, **6** (1990) 119–27.
8. Cheng, Y. B. & Thompson, D. P., Aluminium-containing nitrogen melilite phases. *J. Am. Ceram. Soc.*, **77** (1994) 143–48.
9. Werner, P. -E., A Fortran program for least-squares refinement of crystal-structure cell dimensions. *Ark. Kemi.*, **31** (1969) 513–6.
10. Sun, W. Y. & Yan, D. S. (ed. Yen, T. S.), Phase relationships in quasi-systems R_2O_3–AlN–Al_2O_3 (R = Ce, Pr, Nd, Sm). *Science in China (Series A)*, **34** (1991) 105–15.
11. Sun, W. Y., Huang, Z. K., Tien, T. Y. & Yen, T. S., Phase relationship in the system Y–Al–O–N. *Mater. Lett.*, **11** (3,4) (1991) 67–69.
12. Vainshtein, B. K., Fridkin, V. M. & Indenbom, V. L., Crystallochemical radii systems, In *Modern Crystallography II, Structure of Crystals*, ed. B. K. Vainshtein, A. A. Chernov, & L. A. Shuvalov, Springer, Berlin, Heidelberg, 1982, pp 78–81.